Nuclear Engineering and Technology 55 (2023) 2873–2878

Contents lists available at ScienceDirect

Nuclear Engineering and Technology

journal homepage: www.elsevier.com/locate/net

Original Article

Development and evaluation of a compact gamma camera for radiation monitoring

Dong-Hee Han [a], Seung-Jae Lee [b], Hak-Jae Lee [c], Jang-Oh Kim [a], Kyung-Hwan Jung [a], Da-Eun Kwon [a], Cheol-Ha Baek [a, *]

[a] Kangwon National University, Republic of Korea
[b] Dongseo University, Republic of Korea
[c] ARALE Laboratory Co., Ltd., Republic of Korea

ARTICLE INFO

Article history:
Received 26 February 2023
Received in revised form
13 April 2023
Accepted 19 April 2023
Available online 19 June 2023

Keywords:
Radiation monitoring
Gamma imaging
Performance tests
^{99m}Tc
Miniaturization

ABSTRACT

The purpose of this study is to perform radiation monitoring by acquiring gamma images and real-time optical images for ^{99m}Tc vial source using charge couple device (CCD) cameras equipped with the proposed compact gamma camera. The compact gamma camera measures 86 × 65 × 78.5 mm^3 and weighs 934 g. It is equipped with a metal 3D printed diverging collimator manufactured in a 45° field of view (FOV) to detect the location of the source. The circuit's system uses system-on-chip (SoC) and field-programmable-gate-array (FPGA) to establish a good connection between hardware and software. In detection modules, the photodetector (multi-pixel photon counters) is tiled at 8 × 8 to expand the activation area and improve sensitivity. The gadolinium aluminium gallium garnet (GAGG) measuring 0.5 × 0.5 × 3.5 mm^3 was arranged in 38 × 38 arrays. Intrinsic and extrinsic performance tests such as energy spectrum, uniformity, and system sensitivity for other radioisotopes, and sensitivity evaluation at edges within FOV were conducted. The compact gamma camera can be mounted on unmanned equipment such as drones and robots that require miniaturization and light weight, so a wide range of applications in various fields are possible.

1. Introduction

Gamma imaging is defined as a technology that detects gamma-rays (as electrical signals through a detection module), processes, analyzes, and displays them. It is used for environmental monitoring in various fields such as radioactive contamination, inspection of loss and leakage of sources, and prevention of nuclear terrorism. With the continuous development of advanced unmanned equipment in recent years, weight reduction and miniaturization of mountable devices have become necessary. Relevant research is being conducted by various research groups [1–4]. F. Carrel et al., who developed the GAMPIX gamma imaging device for radiological safety and homeland security, used coded-aperture masks and 1.0 mm CdTe substrate to monitor ^{60}Co, ^{137}Cs, and ^{241}Am sources. The device weighs about 1 kg and MCNPX was utilized to develop decoding algorithms such as EM algorithm [5,6]. Y. Hu et al. used compact industrial monitoring gamma cameras with coded-aperture masks and GAGG (Ce) scintillator, with target nuclides of ^{99m}Tc, ^{18}F, and ^{137}Cs [7].

Conventional gamma cameras have been manufactured and used in combination with a large, heavy, high-voltage photomultiplier tube (PMT) and a single inorganic scintillator [8]. Subsequently, with the introduction of pixelated scintillators, position sensitive PMT (PSPMT), and silicon PM (SiPM), gamma images with excellent resolution were obtained. Equipment miniaturization was also made possible through the use of multiple functional element integrated circuits. Furthermore, a number of studies have been conducted to combine monitoring images with interlinkable optical cameras to protect radiation workers by visualizing the exact location of the source while conducting radiation monitoring over a wide area [9,10].

A collimator that selectively reaches the detection module is used to determine the source's location. A pinhole collimator is capable of obtaining high resolution images over a wide field-of-view required for monitoring activities, but it is a major drawback in terms of limited sensitivity, poor signal-to-noise ratio, and performance differences dependent on hole size [11,12]. In the case of a

* Corresponding author.
E-mail address: baekch@kangwon.ac.kr (C.-H. Baek).

https://doi.org/10.1016/j.net.2023.04.029

coded-aperture type including ring aperture, penumbra aperture, array, etc., sensitivity can be improved through multiple holes in the masks. At the same time, spatial resolution can be maintained, and clear images can be yielded as output using various algorithms using the specific distribution of the hole array [13]. However, disadvantages such as complexity due to the use of point diffusion and the use of difficult filters or reconstruction algorithms have been reported in the decoding process [14].

The diverging collimator has high efficiency and excellent resolution, but its physical structure is complex and its manufacture according to parameters is limited. Recently, with the development of the direct metal laser sintering (DMLS) technique among 3D printing technologies, output using tungsten powder, which is denser than conventional lead material, has become possible. We manufactured the diverging collimator and attached it to the gamma camera [15].

Therefore, the purpose of this study is to conduct a performance evaluation of radioactive isotopes using a compact gamma imaging system combined with an optical camera. Radiation monitoring through a real-time gamma image and optical image combination is also performed.

2. Methods and materials

2.1. Compact gamma camera

A diverging collimator (Collimator height: 15.0 mm, Hole size: 0.7 mm, Septal thickness: 0.1 mm, Field of view: 45°) optimized for monitoring ^{99m}Tc radioactive point sources was manufactured using DMLS 3D printing technology as shown in Fig. 1. The collimator was mounted on the gamma camera detection module and the cube shape shown in Fig. 1 covers the detection module.

The components of the detection module are vital in the miniaturization of the gamma camera system. LYSO, LSO, which are high atomic number scintillators, were used in radiation monitoring, and high signal-to-noise and good energy resolution were possible. In addition, CsI, NaI, etc. with moderate density and high light yield have been used [16,17]. We determine GAGG scintillator with physical properties as shown in Table 1, especially with high density, light yield, and maximum emission wavelength close to 450 nm of SiPM's peak sensitivity wavelength. The pixel size of the GAGG scintillator is 0.5 × 0.5 × 3.5 mm^3, arranged at 38 × 38, wound with Teflon, and attached to a 1.0 mm thick light pipe.

The GAGG was attached to a multi-pixel photon counter (MPPC, S13361-3050AE-08, Hamamatsu, Japan), which is an 8 × 8 array tile type. SiPM is small in size, light in weight, and has excellent spatial resolution for radiographic imaging. It also has excellent hardware compatibility with various circuits. As shown in Fig. 2, noise was minimized by coupling on a plate with a thickness of 5.0 mm of tungsten (about 99% blocked based on 140 keV).

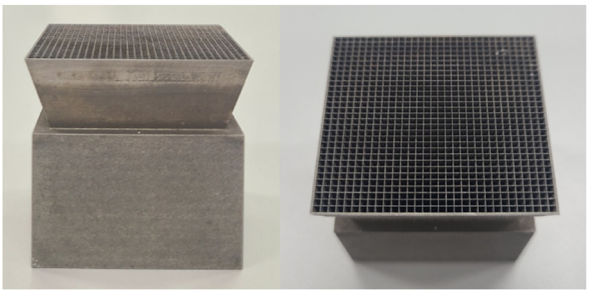

Fig. 1. Diverging-tungsten collimator (Advanced Technology & Materials Co., Ltd. (ATTL Advanced Materials Co., Ltd., China)).

Table 1
Physical characteristics of gadolinium aluminium gallium garnet scintillator (GAGG).

Density [g/cm^3]	6.63
Light yield [photons/MeV]	46,000
Decay time [ns]	90
Peak emission [nm]	520
Hygroscopic	No

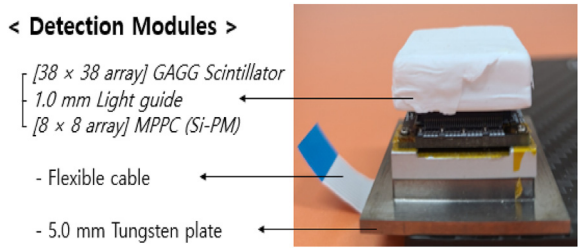

Fig. 2. Detection module components in the gamma imaging system.

Four core circuits that are interlocked with the flexible cable of the detection module, they are combined with a stack type circuit configuration that is optimally developed for signal processing [18]. It consists of a positioning board, a power distribution board, a base board, and a digital acquisition (DAQ) board. A modularized DAQ-based SoC-FPGA provides real-time signal processing flexibility as well as hardware flexibility. The positioning board adjusts the baseline and gain for signals input from the detection module and transmits a differential signal to the analog-to-digital converter (ADC) driver. The power distribution board includes an Ethernet socket for interworking with a laptop, and has a power supply for MPPC (C11204-02, Hamamatsu, Japan) for temperature compensation function required by SiPM. The base board and SoC-FPGA have an SD card for system construction, a 16-channel ADC circuit for operation, a system-on-chip (SoC) that implements various function with a single chip, and a field-programmable-gate-array (FPGA) that easily processes large amounts of data in clock units [18,19].

2.1.1. Intrinsic and extrinsic performance evaluation in experiment and Monte Carlo simulation

Performance evaluation of intrinsic and extrinsic properties and gamma-radiation monitoring activities were conducted. In addition, we simulated the same experimental conditions such as GAGG scintillator in the module, radionuclides, and diverging collimator in Monte Carlo simulation tool GATE v9.0, and then conducted comparative verification with measurements. The radioactive isotopes used were ^{99m}Tc, ^{57}Co, and ^{241}Am.

Uniformity was obtained through each energy spectrum and 2D gamma image using a^{57}Co plane source (REF. DATE: 2021.09.30, Activity: 20 mCi, Half-life: 272 days) and a^{99m}Tc source.

Also, to measure the sensitivity of the system, ^{99m}Tc vial sources were located at distance of 1, 2, 3, and 4 m from the collimator surface and measured for 1 min.

Table 2
Effective area depending on the distance between the imaging system and the radioisotopes.

Distance [cm]	Field of view [cm^2]	Effective area [cm^2]
30	21.0 × 21.0	16.8 × 16.8
50	32.8 × 32.8	26.2 × 26.2
70	44.5 × 44.5	35.6 × 35.6

Table 3
Comparison of normalized system sensitivity with distance in experiments and simulations.

Distance [m]	1	2	3	4
Experiment	1	0.31	0.15	0.09
Simulation	1	0.24	0.11	0.06
Error rate [%]	–	6.69	3.91	2.67

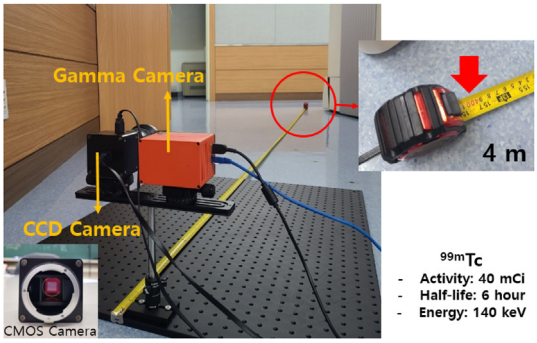

Fig. 3. Developed compact gamma imaging system.

To simultaneously monitor ^{57}Co of about 122 keV and ^{241}Am of about 59.5 keV, this system that is optimized for ^{99m}Tc sources for thyroid treatment and diagnosis was used. The source discrimination ability, i.e., energy resolution according to the energy window adjustment was confirmed.

To verify the sensitivity to remain constant regardless of the location of the source within the effective area, which is one of the advantages of the diverging collimator, the sensitivity was measured by moving the source equally on the X-axis as shown in Table 2. The vial source was moved at regular intervals of 2.5 cm from the center to the X-axis at a distance of 30 cm from the collimator surface. The evaluation processes were conducted by moving at 4 cm intervals for a 50 cm distance and 5 cm intervals for a 70 cm distance. At this time, the effective area is defined as 80% of the field of view, while the area is calculated according to the collimator angle of 45°.

2.1.2. Radiation monitoring with optical and gamma images

For high-resolution real-time image, a CMOS camera (MC089CG-SY, XIMEA, Germany) with 8.9 million pixels of approximately 3.45 μm size and 43 fps performance was selected. The combined compact gamma imaging system is shown in Fig. 3.

We obtained a comprehensive monitoring images for 1 min by placing a ^{99m}Tc vial source of 40 mCi on the 1, 2, 3, and 4 m from the front axis. In addition, two sources in the field of view were randomly located at different distances to monitor the images according to system sensitivity.

3. Results

3.1. Intrinsic and extrinsic performance evaluation in experiment and Monte Carlo simulation

As shown in Fig. 4, the energy spectrum was obtained using ^{99m}Tc and ^{57}Co. The gamma-ray energy peak point was clearly confirmed by controlling the gain value, and an intrinsic uniformity image was confirmed through gamma images.

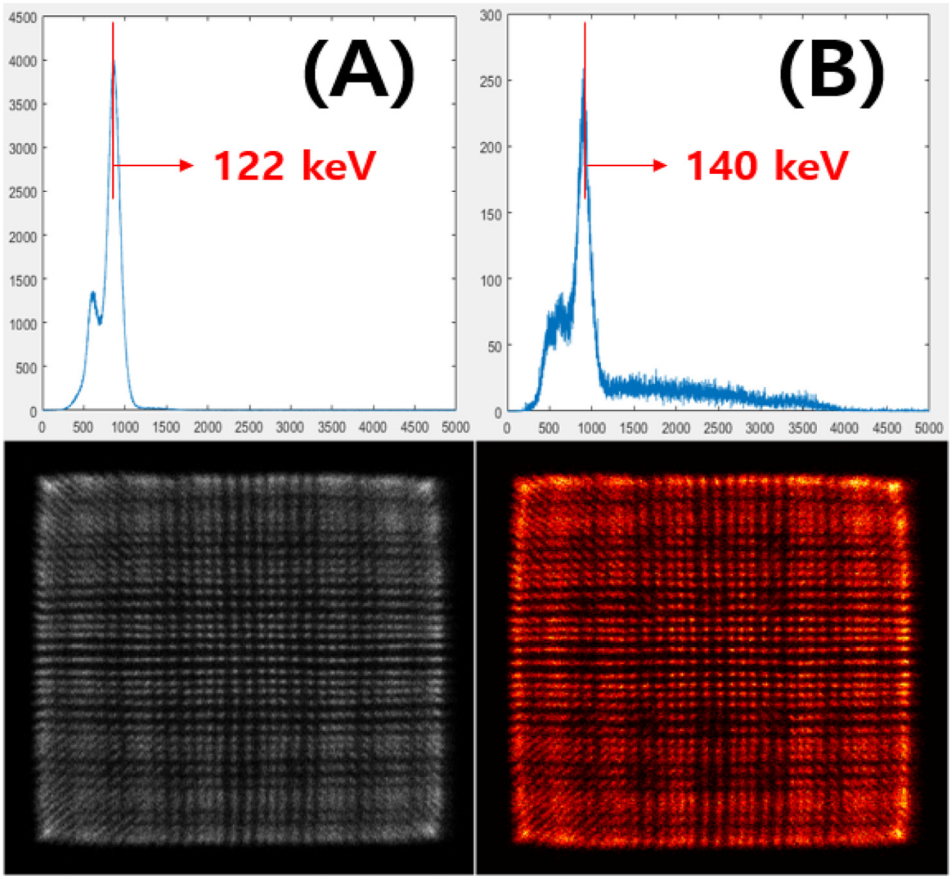

Fig. 4. Intrinsic uniformity and energy spectrum for (A) ^{57}Co (B) ^{99m}Tc.

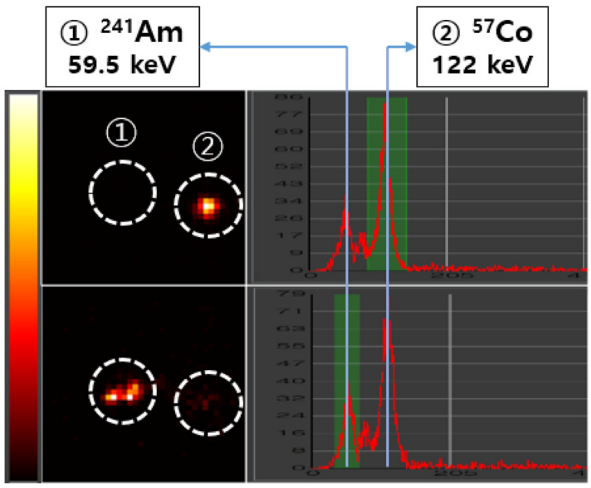

Fig. 5. Variation of gamma images output according to energy window range.

As shown in Table 3, the normalized sensitivity of the system according to the source distance was measured and performed for 1 min through experiments and simulations. Normalization was applied for relative comparison and an average error rate of less than 5% was confirmed.

The energy spectrum for ^{241}Am and ^{57}Co sources were confirmed, and the variation in gamma images according to the energy window range was obtained as shown in Fig. 5.

Through experiment and Monte Carlo simulations, constant sensitivity within the effective area was verified. It showed an average error rate of less than about 2% at distances of 30, 50, and 70 cm as shown in Fig. 6. It was confirmed that the sensitivity rapidly decreased in the area outside the edge of the effective area.

3.2. Radiation monitoring with optical and gamma images

Radiation monitoring activity was performed by configuring a compact gamma imaging system that combines gamma images and real-time optical images. Through the pixel concentration of the segmentation map, it was confirmed that system sensitivity and noise decreased as the distance increased (see Fig. 7).

In addition, when gamma imaging monitoring was performed on randomly located vial sources, the source location was accurately detected. High sensitivity was identified in relatively close sources (see Fig. 8).

4. Discussion

This study sought to conduct various performance evaluations and radiation monitoring of radioactive sources using a compact gamma imaging system. In a previous study, collimator manufacturing was carried out with DMLS 3D printing technique, taking into account the parameters of diverging collimator optimized for ^{99m}Tc [15]. A gamma camera was also constructed using a modularized circuit configuration that allows real-time electrical signals to be processed with maximum efficiency through a DAQ-based SoC-FPGA and has excellent hardware compatibility with

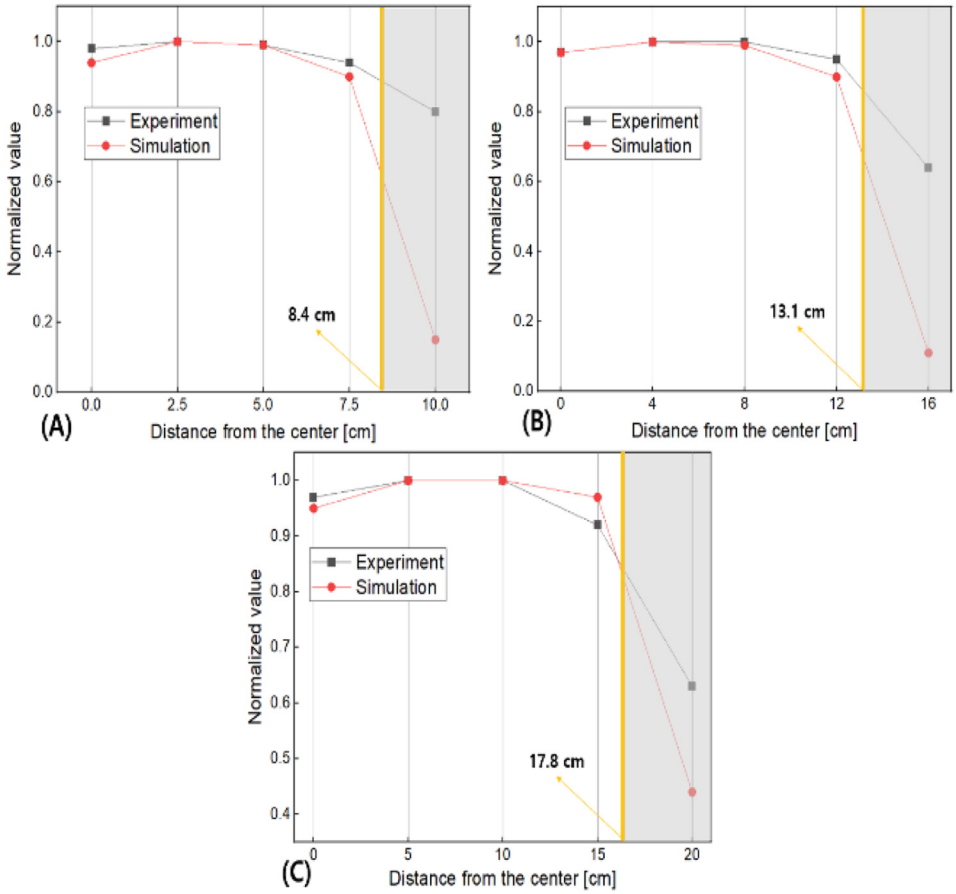

Fig. 6. Sensitivity according to the location of radioactive source in experiments and Monte Carlo simulation (GATE). (A) 30 cm (B) 50 cm (C) 70 cm

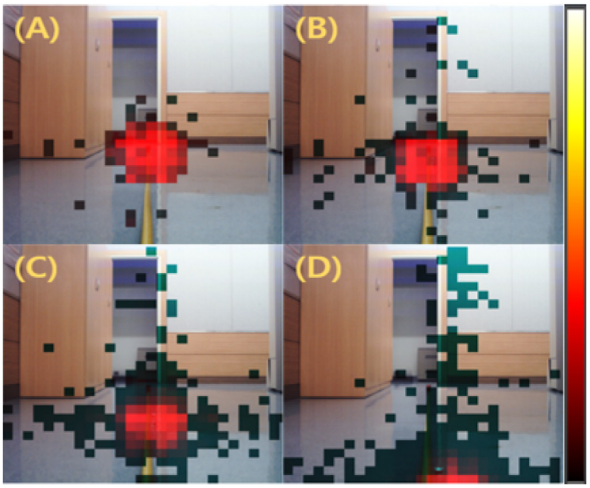

Fig. 7. Comprehensive monitoring images depending on the distance of the ^{99m}Tc vial source from the gamma imaging system (A) 4 m (B) 3 m (C) 2 m (D) 1 m.

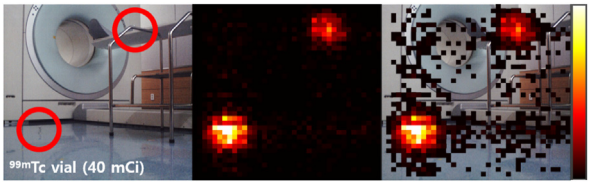

Fig. 8. Detection images of a^{99m}Tc vial source hidden in the medical room at random.

other devices [18].

In the case of the energy spectrum, the peak point of each source could be identified according to the control of the gain value, but in the uniformity image, the signal was blurred due to the pile-up effect in the edge region. It has been suggested that this can be overcome by acquiring an image after being separated from the gamma camera by a certain distance. In addition, intrinsic system sensitivity was measured and compared through experiments and Monte Carlo simulation. Although the theoretical inverse-square law was not shown, an average error range of less than 5% was confirmed, and extrinsic system sensitivity measurement is required in the future. By checking the energy spectrum for ^{241}Am (about 59.5 keV) and ^{57}Co (about 122 keV) sources, we propose the applicability for monitoring areas where radiation fields are formed by multiple radioactive sources using the corresponding gamma imaging system.

Radiation monitoring of randomly hidden vial sources in the field of view was performed, and real-time combined gamma and optical images were obtained. Experiments were conducted mainly in terms of sensitivity using a relatively thin GAGG scintillator (3.5 mm thick) in the detection modules. A clear radiation image research is needed to remove noise depending on the signal-to-noise ratio (SNR) through energy window control. In addition, monitoring conditions and distance from the radioactive sources should be considered.

5. Conclusion

Our researchers proposed a novel compact gamma imaging system capable of performing radiation monitoring over a wide field-of-view. The performance was verified through comparative analysis of the experiment and Monte Carlo simulation. The location of the source can be accurately identified with excellent sensitivity and progressive performance. The imaging system was equipped with an optimized diverging collimator aimed at relatively low-energy gamma sources, which are mainly used in the medical field. It can have a wide array of applications including preventing terrorism, detecting lost isotopes, and preventing workers' exposure. Further research will be conducted by developing additional devices and mounting unmanned equipment for main monitoring nuclides in industries that emit high-energy gamma rays such as ^{131}I and ^{137}Cs.

Declaration of competing interest

The authors declare that they have no known competing financial interests or personal relationships that could have appeared to influence the work reported in this paper.

Acknowledgement

This research was supported by the National Research Foundation of Korea (NRF) funded by the Ministry of Education, Science and Technology (2020R1C1C1004584).

References

[1] J.E. Lees, S.L. Bugby, A.P. Bark, D.J. Bassford, P.E. Blackshaw, A.C. Perkins, A hybrid camera for locating sources of gamma radiation in the environment, J. Instrum. 8 (2013), P10021.
[2] G. Amoyal, V. Schoepff, F. Carrel, M. Michel, N.B. de Lanaute, J.C. Angelique, Development of a hybrid gamma camera based on Timepix3 for nuclear industry applications, Nucl. Instrum. Methods Phys. Res. B 987 (2021), 164838.
[3] C. Zhao, B. Zhu, M. Zhao, Q. Chen, Z. Wang, R. Zhou, C. Yang, Development of a modular high-sensitivity high-uniformity gamma camera for radiation monitoring applications, Nucl. Instrum. Methods Phys. Res. B 1003 (2021), 165340.
[4] C.H. Baek, S.J. An, H.I. Kim, S.W. Kwak, Y.H. Chung, Development of a pinhole gamma camera for environmental monitoring, Radiat. Meas. 59 (2013) 114–118.
[5] F. Carrel, R.A. Khalil, P. Blot, K. Boudergui, S. Colas, M. Gmar, F. Lemasle, N. Saurel, V. Schoepff, H. Toubon, GAMPIX: a new generation of gamma camera for hot spot localization, in: Proceddings of the ISOE Conference, 2010.
[6] F. Carrel, R.A. Khalil, S. Colas, D.D. Toro, G. Ferrand, E. Gaillard-Lecanu, M. Gmar, D. Hameau, S. Jahan, F. Laine, A.S. Lalleman, GAMPIX: a new gamma imaging system for radiological safety and homeland security purposes, in: 2011 IEEE NSS Conference Record, 2011, pp. 4739–4744.
[7] Y. Hu, Z. Lyu, P. Fan, T. Xu, S. Wang, Y. Liu, T. Ma, A wide energy range and 4π-view gamma camera with interspaced position-sensitive scintillator array and embedded heavy metal bars, Sensors 23 (2023) 953.
[8] W. Siman, S. Cheenu Kappadath, Performance characteristics of a new pixelated portable gamma camera, Med. Phys. 39 (2012) 3435–3444.
[9] H.I. Kim, S.J. An, Y.H. Chung, S.W. Kwak, Development of an all-in-one gamma camera/CCD system for safeguard verification, J. Kor. Phys. Soc. 65 (2014) 2013–2016.
[10] D.M. Im, J.H. Jung, Y. Choi, D. Jang, D. Kim, Y.H. Kim, J.H. Kim, Development of compact coded aperture gamma camera for radiation monitoring in nuclear facility, in: 2017 IEEE NSS/MIC, 2017, pp. 1–3.
[11] J. Islamian, A. Azazrm, B. Mahmoudian, E. Gharapapagh, Advances in pinhole and multi-pinhole collimators for single photon emission computed tomography imaging, World J. Nucl. Med. 14 (2015) 3–9.
[12] F. Garibaldi, R. Accorsi, M.N. Cinti, E. Cisbani, S. Colilli, F. Cusanno, G. De Vincentis, A. Fortuna, R. Fratoni, B. Girolami, F. Ghio, Small animal imaging by single photon emission using pinhole and coded aperture collimation, IEEE Trans. Nucl. Sci. 52 (2005) 573–579.
[13] H. Zhang, B. Zhong, H. Shen, L. Cheng, J. Li, Research on a Monte Carlo simulation method of neutron coded-aperture imaging, Nucl. Sci. Eng. 196 (2022) 1236–1246.
[14] R. Zhang, X. Tang, P. Gong, P. Wang, C. Zhou, X. Zhu, D. Liang, Z. Wang, Low-noise reconstruction method for coded-aperture gamma camera based on multi-layer perceptron, Nucl. Eng. Technol. 52 (2020) 2250–2261.
[15] J.H. Won, D.H. Han, S.J. Lee, C.H. Baek, Development of a gamma camera with a diverging collimator using DMLS 3D printing, Jpn. Mag. 25 (2020) 606–613.
[16] M. Jeong, B. Van, B.T. Wells, J.D. Lawrence, M.D. Hammig, Comparison between pixelated scintillators: CsI (Tl), LaCl 3 (Ce) and LYSO (Ce) when coupled

to a silicon photomultipliers array, Nucl. Instrum. Methods Phys. Res. B 893 (2018) 75–83.
[17] K. Nakanishi, S. Yamamoto, J. Kataoka, Performance comparison of finely pixelated LYSO-and GAGG-based Si-PM gamma cameras for high resolution SPECT, Nucl. Instrum. Methods Phys. Res. B 872 (2017) 107–111.
[18] B. Yu, S. Bae, C.H. Baek, J.Y. Yeom, K. Lee, H. Lee, Development of compact gamma camera using SoC-FPGA based modularized DAQ, in: 2019 IEEE NSS/MIC, 2019, pp. 1–3.
[19] G. Saldana-Gonzalez, H. Salazar-Ibarguen, O.M. Bravo, E. Moreno-Barbosa, 2D image reconstruction with a FPGA-based architecture in a gamma camera application, in: 2010 20th CONIELECOMP, 2010, pp. 102–105.